Structural Phase Transitions and Three-Dimensional Magnetic Ordering in the Nd_2NiO_4 Oxide

1990 Europhys. Lett. 11 261

(http://iopscience.iop.org/0295-5075/11/3/013)

EUROPHYSICS LETTERS 1 February 1990

Europhys. Lett., 11 (3), pp. 261-268 (1990)

Structural Phase Transitions and Three-Dimensional Magnetic Ordering in the Nd_2NiO_4 Oxide.

J. RODRÍGUEZ-CARVAJAL (*), M. T. FERNÁNDEZ-DÍAZ (*), J. L. MARTÍNEZ (*)
F. FERNÁNDEZ (**) and R. SAEZ-PUCHE (**)

(*) *Institut Laue Langevin, 156X - F-38042 Grenoble Cedex, France*
(**) *Departamento de Química Inorgánica, Facultad de Ciencias Químicas Universidad Complutense - E-28040 Madrid, Spain*

(received 16 October 1989; accepted in final form 8 December 1989)

PACS. 75.25 – Spin arrangements in magnetically ordered materials (neutron studies, etc.).

Abstract. – Neutron diffraction on polycrystalline samples of stoichiometric Nd_2NiO_4 shows a complex structural and magnetic behaviour as a function of temperature. The room temperature (RT) phase is orthorhombic (*Bmab*) and Ni^{2+} ions are 3D antiferromagnetically ordered ($T_N \approx 320$ K), with a propagation vector $\boldsymbol{k} = [100]$ and spins oriented parallel to the propagation vector, *i.e.* along the *a*-axis. The magnetic structure can be described as a g_x mode (Shubnikov group $B_P mab'$). The magnetic moment for Ni^{2+} is $1.57\mu_B$ at 160 K. The system undergoes a structural phase transition from orthorhombic to tetragonal ($P4_2/ncm$) at $T_1 \approx 130$ K. The tetragonal phase allows the existence of a ferromagnetic component along *c*-axis in the Ni^{2+} spin structure, the magnetic structure can be described either as a $g_x c_y f_z$ mode (Shubnikov group $Pc'c'n$) or as a $g_x + c_y f_z$ mode (Shubnikov group $P4_2/nc'm'$). At a temperature as high as 70 K the polarization of the Nd^{3+} ions becomes noticeable. At low temperature ($T_N \approx 8$ K) Nd^{3+} ions cooperative order takes place with a magnetic moment of $3.2\mu_B$ at 1.5 K and a magnetic structure belonging to the same Shubnikov group (either $Pc'c'n$ or $P4_2/nc'm'$). Fully oxidized samples of $Nd_2NiO_{4+\delta}$ as obtained in air atmosphere, seems to be also orthorhombic at RT and do not show static magnetic order or structural phase transitions between 1.5 K and 300 K. Partially oxidized samples ($\delta = 0.04$) are also orthorhombic at RT, and show a similar magnetic behaviour as stoichiometric ones, but no structural phase transition at low temperatures is observed.

Introduction. – Recently, a new family of cuprate superconductors has been reported with the general formula $R_{2-x}C_xCuO_4$, with R = Pr, Nd, Sm, Eu and Gd, and C = Ce and Th [1, 2]. These materials are important because they show electron conductivity and have a different crystallographic structure from the well-known La_2CuO_4-type (orthorhombic). The structure of these rare-earth cuprates is tetragonal (*I4/mmm*, Nd_2CuO_4-type, often called the *T'* structure), with a square planar arrangement of the Cu-O atoms. This new family shows many new magnetic and structural properties [2, 3], and it seems that coexistence of superconductivity with antiferromagnetic ordering of the rare-earth ions is possible in some cases [4]. There are a few characteristics in common with the R_2CuO_4-family as Oseroff *et al.* [3] pointed out. In particular, a peak in the specific heat at low temperature for some

rare-earth atoms; two sharp peaks in the d.c. magnetization as well as a weak ferromagnetic component. The high-temperature peak in magnetization corresponds to the magnetic ordering of the Cu sublattice, as in La_2CuO_4. The low-temperature peak is still not well understood, and varies with the rare-earth atom and stoichiometry. In some cases, the rare earth orders antiferromagnetically, *e.g.*, in compounds with Nd, Sm and Gd [2]. But, the origin of this peak could also be related to a spin reorientation of Cu atoms [3]. Recent neutron diffraction experiment on Nd_2CuO_4 [5] have shown the existence of a complex magnetic behaviour below RT, *e.g.*, five magnetic transitions in this temperature range.

Superconductivity has also been reported in La_2NiO_4 compounds [6]. At present, no independent confirmation of superconductivity in doped La_2NiO_4 has been published, but there is still strong interest in studying the structural, magnetic and electronic properties of nickelates in order to compare their behaviour with the related cuprates. In contrast to the Nd_2CuO_4-type oxides, the nickelates retain the orthorhombic structure [7] derived from the parent *T*-structure (K_2NiF_4-type), with Ni atoms in an octahedral coordination, but also revealing a wide variety of structural and magnetic properties [8]. In spite of the growing understanding of La_2NiO_4, very few information is still available on related R_2NiO_4 with R = Pr and Nd.

In this letter we present a general survey of the neutron diffraction experiments carried out on three samples of Nd_2NiO_4 with different oxygen stoichiometry over a wide range of temperatures. In particular, we show that the 3*d* cation orders antiferromagnetically; we present experimental evidence of structural phase transitions and finally the magnetic configuration of the rare-earth ions at low temperature is described. Theoretical group representation analysis of the different types of magnetic structures, as well as further details concerning the crystallography and microstrains induced by the structural phase transition will be published elsewhere.

Experimental. – Nd_2NiO_4 polycrystalline samples were synthesized using standard ceramic methods. The stoichiometric compounds was obtained by reducing the oxidized precursors in flowing dry hydrogen at 510 K [9]. The sample presents a brown colour. Stoichiometric samples are insulators, while oxidized samples are semiconductors with a gap of roughly 0.05 eV at RT.

Neutron diffraction experiments were carried out at the High Flux Reactor of the Institut Laue Langevin in Grenoble, on the powder diffractometers D1B and D2B, with neutrons wavelengths of 2.52 Å and 1.59 Å, respectively. Standard cryostats were used in the low-temperature range. A furnace with vanadium resistor was used for the high-temperature set-up. Three kinds of samples were used in the neutron diffraction experiments: stoichiometric samples (S), fully oxidized samples (O) annealed in air at 1450 K, and a partially oxidized sample (P) obtained from sample (O) in the course of a high-temperature neutron diffraction experiment performed under vacuum ($pO_2 \approx 10^{-4}$ Torr). The excess oxygen (δ) in $Nd_2NiO_{4+\delta}$ calculated from the neutron diffraction data for the P sample is $\delta = 0.04$.

Results and discussion. – Figure 1 shows the RT diffraction patterns of the three different samples (O, P, and S) of Nd_2NiO_4, as obtained on D1B. All reflections can be indexed in the space group *Bmab*, except the weak magnetic reflections (011) and (102) of sample S, which are still present at RT (the Ni sublattice becomes ordered at $T_N \approx 320$ K), and some small peaks of the O sample. The cell parameters at RT of the three samples are shown in fig. 1. It is remarkable that the orthorhombic strain (defined as $s = 2(b - a)/(a + b)$) is higher in the O-sample than in the P-sample. In the sample S, the strain is even higher than in O.

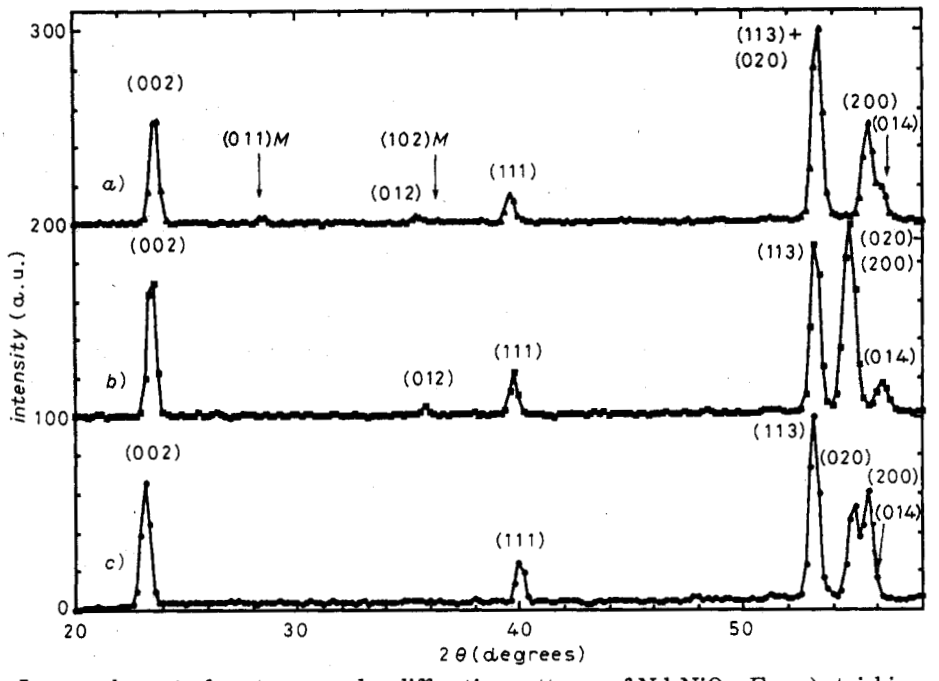

Fig. 1. – Low angle part of neutron powder diffraction patterns of Nd_2NiO_4. For *a*) stoichiometric (S) ($a = 5.3876$ Å, $b = 5.5883$ Å, $c = 12.135$ Å), *b*) partially oxidized (P) ($a = 5.4487$ Å, $b = 5.4664$ Å, $c = 12.206$ Å) and *c*) fully oxidized (O) ($a = 5.3821$ Å, $b = 5.4440$ Å, $c = 12.360$ Å) at room temperature (RT), $T = 300$ K.

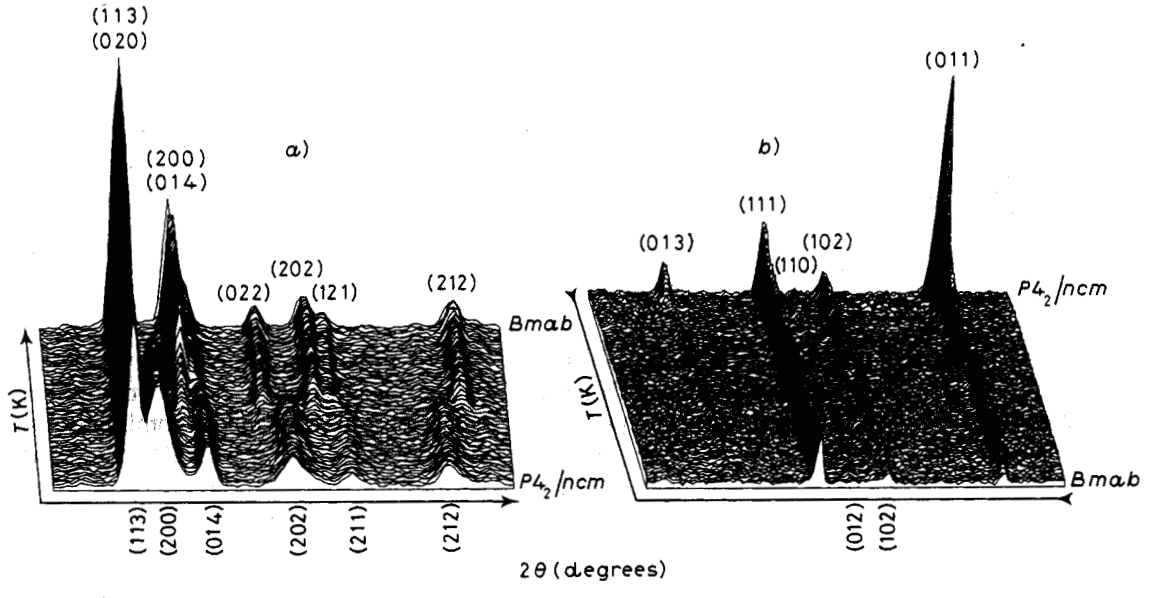

Fig. 2. – 3D plots (intensity *vs.* 2θ and temperature) in stoichiometric Nd_2NiO_4. *a*) Bragg peaks showing the structural phase transition at $T_1 = 130$ K ($50 < \theta < 70$ degrees; $1.5 < T < 300$ K); *b*) magnetic reflections showing the progressive ordering of Nd sublattice ($25 < \theta < 45$ degrees; $1.5 < T < 300$ K) $\lambda = 2.52$ Å (D1B).

In fig. 2 we present, for the sample S, 3D-plots of the scattered intensity, I, *vs.* 2θ and T, in two selected angular ranges. In fig. 2*a*) the first-order phase transition from an orthorhombic to a tetragonal structure at $T = 130$ K can be observed. Figure 2*b*) shows the increase of the magnetic reflections due to the progressive magnetic ordering of Nd^{3+} cations below 80 K. The same kind of experiment has been performed on the samples P and O. In the first case we observed the 3D magnetic ordering of Ni^{2+} at 82 K and the Nd ordering at lower temperature ($T \approx 8$ K), but no structural phase transition takes place. In the second case neither magnetic ordering nor structural phase transitions were found.

Crystal and magnetic structure of stoichiometric Nd_2NiO_4 ($130 < T < 320$ K).

Rietveld refinement of the high-resolution (D2B) diffraction pattern of sample S at 160 K gives the results presented in table I. The spin arrangement of Ni^{2+} at this temperature was

TABLE I. – *Results of Rietveld refinements on* Nd_2NiO_4.

Temperature (K) Space Group	330 (D1B) *Bmab*	150 (D2B) *Bmab*	1.5 (D2B) $P4_2/ncm$
a(A)	5.3876(5)	5.37325(9)	5.480(1)
b(A)	5.5883(5)	5.5913(1)	5.480(1)
c(A)	12.135(1)	12.0976(2)	12.057(3)
strain	0.03657	0.03899	0
Ni(0 0 0)	—	—	—
Nd	(0 *y z*)	(0 *y z*)	(*x x z*)
y	−0.015(1)	−0.0173(3)	−0.0121(5)
z	0.3632(3)	0.3630(1)	0.3641(2)
O1(1/4 1/4 z)			
z	−0.0179(6)	−0.0177(2)	−0.0298(6)
O2	(0 *y z*)	(0 *y z*)	(*x x z*)
y	0.063(1)	0.0652(3)	0.0508(5)
z	0.1794(6)	0.1806(2)	0.1785(5)
O1′	—	—	(3/4 1/4 0)
Moment (μ_B) total	0	1.57(5)	3.2(Nd) 1.59(Ni)
In-plane component	—	—	2.87(4)(Nd) 1.54(5)(Ni)
Out-of-plane component	—	—	1.0(2)(Nd) 0.4(2)(Ni)
R-Bragg(%)	4.36	6.46	7.33

Numbers in parenthesis indicate standard deviation in the last digit.

analysed using the macroscopic theory of Bertaut [10]. Numbering the Ni sublattices as $Ni_1(000)$, $Ni_2(1/2\,0\,1/2)$, $Ni_3(0\,1/2\,1/2)$ and $Ni_4(1/2\,1/2\,0)$, the basis vectors of the one-dimensional representation of *Bmab* can be constructed from the following linear combinations: $f = s_1 + s_2 + s_3 + s_4$, $g = s_1 - s_2 + s_3 - s_4$, $c = s_1 + s_2 - s_3 - s_4$ and $a = s_1 - s_2 - s_3 + s_4$. The magnetic structure is described by the mode g_x ($B_P mab'$ magnetic group) and the corresponding representation allows no ferromagnetic component [11]. The conditions ruling the existence of the magnetic reflections for mode g are: $h = 2n$, k and l odd or $h = 2n + 1$, k and l even. In all other cases the magnetic intensity is zero. In this model the first and most intense reflection is (0 1 1) as it is observed. In contrast with the case of La_2CuO_4, whose magnetic structure is described by the mode $g_y a_z$ ($a_z \approx 0$, $B_P m' a' b'$), in Nd_2NiO_4, the spin direction coincides with the tilt axis of Ni octahedra (see inset *b*) of fig. 3) as in La_2NiO_4 [11]. The origin of this magnetocrystalline anisotropy could be either dipolar or a result of the single-

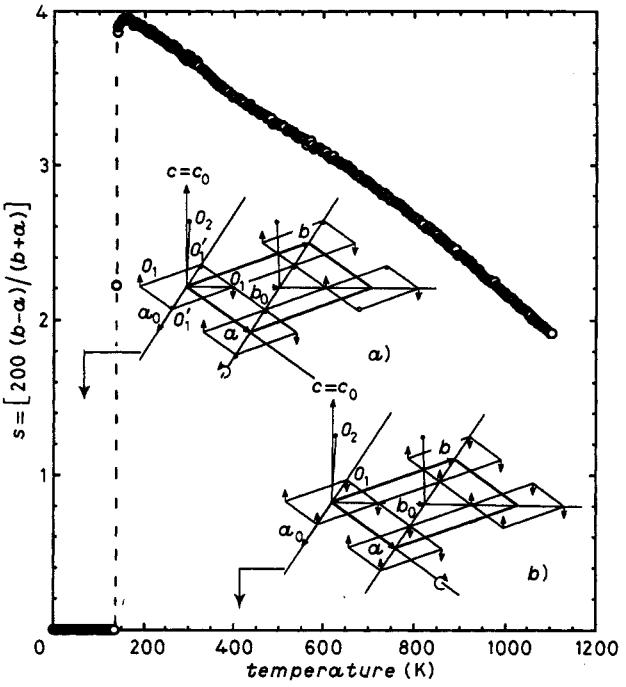

Fig. 3. – Temperature dependence on the orthorhombic strain $s = 2((b - a)/(a + b))$ in stoichiometric Nd_2NiO_4. Inset *a*) gives a schematic illustration of the Ni octahedra tilts at low temperature ($P4_2/ncm$). Inset *b*) shows the Ni octahedra tilts in the orthorhombic phase (*Bmab*). Small arrows indicate the displacement of the oxygen atoms with respect to their position in the parent high-temperature phase ($I4/mmm$), with cell parameters a_0, b_0, c_0. Circular arrows indicate the tilt axis.

ion anisotropy. The magnetic moment at 160 K is $1.57\mu_B$ close to the corresponding value in La_2NiO_4 [11, 12]. The Ni sublattice spin structure is schematically illustrated in fig. 4*c*).

Structural phase transition and magnetic structure of Ni *sublattice* ($1.5 < T < 130$ K).

The structural transition in the S sample is clearly observed in fig. 3, where the orthorhombic strain is represented *vs.* temperature. At 130 K, the system undergoes a first-order phase transition from orthorhombic (*Bmab*) to tetragonal ($P4_2/ncm$). At high temperature, the system tends to transform continuously to the tetragonal (*T*) parent structure ($I4/mmm$). In Nd_2NiO_4 the extrapolated high-temperature transition is 1896 K, which is in fact higher than the melting point of the compound. In the O sample the transition to a tetragonal phase has been observed at about 790 K. The conditions of the experiment (high temperature and vacuum) caused a transformation to a partially reduced orthorhombic phase, due to a progressive loss of oxygen at a constant temperature of 1100 K. A similar sequence of phase transitions has actually been observed in La_2NiO_4 [8, 11] and $(La, Ba)_2CuO_4$ [13]. The influence of these structural changes on the superconducting properties has not been elucidated yet. As in the case of La_2NiO_4, the low-temperature structural transition in stoichiometric Nd_2NiO_4 is associated with a sudden rotation of the Ni octahedra (see inset in fig. 3). This sequence of phase transitions is well known in the layered perovskite structure and some theoretical works within the framework of Landau's theory have been reported [14]. The value of the orthorhombic strain at 150 K (maximum distortion) is almost 0.040, *i.e.* two to three times larger than in the case of La_2NiO_4, where

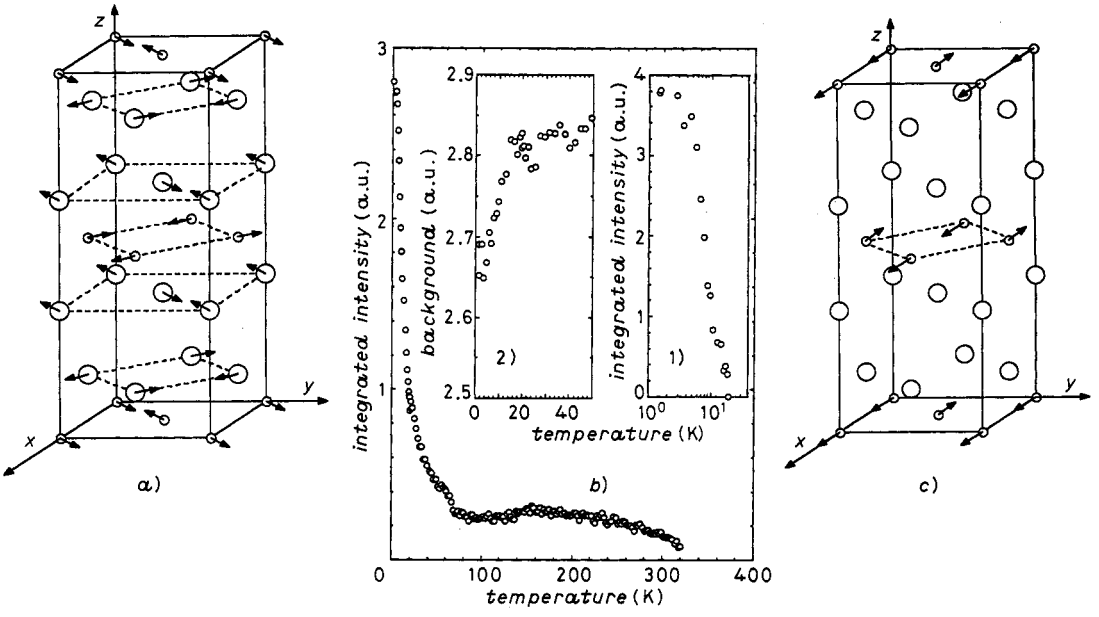

Fig. 4. – *a*) Magnetic structure of stoichiometric Nd_2NiO_4 below 4 K. ○ Ni, ○ Nd. *b*) Temperature variation of the (0 1 1) integrated intensity in Nd_2NiO_4. Inset 1) shows the temperature for the (0 1 3) magnetic reflection. Inset 2) displays the background in the vicinity of the (0 1 1) reflection *vs.* temperature. *c*) Schematic representation of the magnetic structure (nickel sublattice only) in the temperature range 130 K to 320 K. ○ Ni, ○ Nd.

maximum the strain is 0.017 [8], or in $(LaBa)_2CuO_4(0.007)$ [13]. In the case of Nd_2NiO_4 the structural change is very abrupt, as expected for a first-order phase transition. The structure refinement of the low-temperature high-resolution powder patterns using the Rietveld method, is complicated because the phase transition is accompanied by the appearance of strong microstrain which induce a very marked anisotropic broadening of the Bragg reflections. In a first approximation, one can handle this anisotropic broadening by dividing the reflections into two sets: sharp reflections of the *hhl*-type, and broad ones of the general *hkl*-type. This is the approach we have used to refine the low-temperature diffraction patterns. However, a more physical model is needed to solve the peculiar microstructure created by the phase transition. Further details are beyond the scope of this letter.

The influence of this structural transition on the magnetic structure is to enable the anisotropic exchange to create a ferromagnetic component along the *c*-axis. The temperature dependence of the integrated intensity of the (0 1 1) magnetic reflection is shown in fig. 4*b*). The spin structure changes in the range within 130 K and 70 K as indicated by the decrease of I_{011} in the range within 130 K and 70 K. The ferromagnetic component created at 130 K is allowed for the one-dimensional representation of $Pccn$ and $P4_2/ncm$ with the basis functions: $g_x c_y f_z$ (Shubnikov group $Pc'c'n$) and $g_x + c_y f_z$ (Shubnikov group $P4_2/nc'm'$). The notation $g_x + c_y$ means that x and y spin components are coupled so that $|s_{ix}| = |s_{iy}|$. Neutron powder diffraction is unable to distinguish between these two possibilities. However, taking into account the fact that the exchange integral between Ni atoms belonging to different perovskite slabs must be small, and considering the origin of the anisotropy to be due to the single ion, it is very likely that main spin components were along the tilt axis of octahedra (see inset *a*) of fig. 3). As this axis is rotated by 90 degrees between adjacent planes along

the *c*-axis, the tetragonal symmetry ($P4_2/nc'm'$) for the magnetic structure is more likely the good model.

The onset of magnetic ordering on Nd *sublattice* ($1.5 < T < 80$ K).

Ni^{2+} cations polarize the Nd sublattice by a local exchange field ($J_{Ni\text{-}Nd} > J_{Nd\text{-}Nd}$). Below 70 K the intensity of magnetic reflection rapidly increases due to the Nd^{3+}-contribution. At low temperature, the Nd sublattice becomes fully ordered ($T_N \approx 8$ K). The onset of the Nd magnetic order is induced by two superimposed effects. In the first stages, when $J_{Ni\text{-}Nd}$ dominates, the Nd^{3+} behaves as paramagnetic cations under a strong local field. The increase of the magnetic reflections is due to the component of the magnetic moment of Nd polarized along the local field. At lower temperatures $J_{Nd\text{-}Nd}$ becomes significant and cooperative ordering is clearly observed in the inset 1) of fig. 4*b*), where the temperature dependence of the integrated intensity of the (0 1 3) magnetic reflection is plotted. This reflection arises mainly from the ordering of the Nd sublattice. Another indication of Nd ordering (inset 2) of fig. 4*b*)) is given by the decrease of the paramagnetic scattering contribution to the background near the (0 1 1) reflection in the same temperature range. When the magnetic moment of Nd is not completely ordered, it contributes to the paramagnetic background of the diffraction pattern. As the magnetic moment becomes three-dimensionally ordered, this contribution disappears and the background decreases below T_N.

The details of the thermal evolution of I_{011} are perfectly reproducible with different samples, but we have not yet analyzed their meaning with respect to spin arrangements of Nd and Ni in the full temperature range. We shall restrict ourselves to the study of the magnetic structure of stoichiometric Nd_2NiO_4 at 1.5 K.

The Nd atoms in the unit cell can be divided into two sets related by a symmetry centre as follows: $Nd_1(0\,0\,z)$, $Nd_2(1/2\,0\,1/2-z)$, $Nd_3(0\,1/2\,1/2-z)$, $Nd_4(1/2\,1/2\,z)$, and $Nd_{1'}(0\,0-z)$, $Nd_{2'}(1/2\,0\,1/2+z)$, $Nd_{3'}(0\,1/2\,1/2+z)$, $Nd_{4'}(1/2\,1/2-z)$. We have neglected the shift of x and y coordinates from the ideal values of the parent T-structure. For each set of four atoms we can use the same labelling of magnetic modes than in the Ni case. The coupling between the two sets results in the following linear combinations: $\boldsymbol{F} = \boldsymbol{F}_1 + \boldsymbol{F}_2$, $\boldsymbol{G} = \boldsymbol{G}_1 + \boldsymbol{G}_2$, $\boldsymbol{C} = \boldsymbol{C}_1 + \boldsymbol{C}_2$, $\boldsymbol{A} = \boldsymbol{A}_1 + \boldsymbol{A}_2$, $\boldsymbol{P} = \boldsymbol{F}_1 - \boldsymbol{F}_2$, $\boldsymbol{Q} = \boldsymbol{G}_1 - \boldsymbol{G}_2$, $\boldsymbol{R} = \boldsymbol{C}_1 - \boldsymbol{C}_2$, $\boldsymbol{L} = \boldsymbol{A}_1 - \boldsymbol{A}_2$. The group representation analysis leads the possible magnetic structures allowed in $Pccn$ or in $P4_2/ncm$. The best results are obtained for the same representation as for the Ni sublattice, *i.e.* $G_xC_yF_z$ (Shubnikov group $Pc'c'n$) or $G_x + C_yF_z$ (Shubnikov group $P4_2/nc'm'$). Powder diffraction data cannot distinguish between the two possibilities. Low-temperature structural and magnetic data are summarized in table I.

The refined magnetic moment for Nd^{3+} is $3.2\mu_B$ at 1.5 K, which is close to the free-ion value ($\mu = gJ$, for a ground state $^4I_{9/2}$) of $3.27\mu_B$. The spin structure at low temperature is illustrated in fig. 4*a*). For the sake of clarity, the ferromagnetic component along the *c*-axis is not represented, but the projection of the Nd moment along the *c*-axis implies an angle of 19.2 degrees.

In conclusion, we have presented a survey of the structural and magnetic properties of Nd nickelates. These properties deserve further investigations in order to get a deeper insight into the microscopic mechanisms responsible for the observed complex behaviour. The low-temperature magnetic ordering and the structural anomaly produce peaks in the specific heat as well as anomalies in the d.c. magnetization [15]. All these properties are strikingly similar to those of Nd_2CuO_4, and a careful comparison between the two materials is needed to clarify the differences. The oxygen stoichiometry is obviously critical for the existence of the low-temperature structural phase transition, as well as on the onset of the three-dimensional magnetic ordering. It is very likely that oxygen excess existing in air-

prepared samples (or slightly reduced ones) creates structural defects which prevent the action of the soft mode responsible for the above-mentioned transition. Moreover, the presence of holes (probably of oxygen-2*p* character) introduces magnetic frustration via random competing magnetic interactions (the interaction Ni^{2+}-O^{-1}-Ni^{2+} will likely be ferromangetic). The breakdown of the 3D static ordering would be a consequence of this frustration. The doping with Sr may produce new effects, varying the balance between different competing couplings, this particular point will be studied in future experiments.

REFERENCES

[1] TOKURA Y., TAKAGI H. and UCHIDA S., *Nature (London)*, **337** (1989) 345.
[2] SEAMAN C. L., AYOUB N. Y., BJORNHOLM T., EARLY E. A., GHAMATY S., LEE B. W., MARKET J. T., NEUMEIER J. J., TSAI P. K. and MAPLE M. B., *Physica C*, **159** (1989) 391.
[3] OSEROFF S., RAO D., WRIGHT F., TOVAR M., VIER D. C., SCHULTZ S., THOMPSON J. D., FISK Z. and CHEONG S.-W., *Solid State Commun.*, **70** (1989) 1150; THOMPSON J. D., CHEONG S.-W., BROWN S. E., FISK Z., OSEROFF S., TOVAR M., VIER D. C. and SCHULTZ S., *Phy. Rev. B*, **39** (1989) 6660.
[4] GHAMATY S., LEE B. W., MARKET J. T., EARLY E. A., BJORNHOLM T., SEAMAN C. L. and MAPLE M. B., *Physica C*, **160** (1989) 217.
[5] SKANTHAKUMAR S., ZHANG H., CLINTON T. W., LI W. H., LYNN J. W., FISK Z. and CHEONG S.-W., *Physica C*, **160** (1989) 124.
[6] ZAKOL Z., SPALEK J. and HONIG J. M., *J. Solid State Chem.*, **79** (1989) 288; ZAKOL Z., SPALEK J. and HONIG J. M., *Solid State Commun.*, **71** (1989) 283; also SPALEK J., ZAKOL Z. and HONIG J. M., *Solid State Commun.*, **71** (1989) 511.
[7] SAEZ-PUCHE R., FERNÁNDEZ F., RODRÍGUEZ-CARVAJAL J., and MARTÍNEZ J. L., *Solid State Commun.*, **72** (1989) 273.
[8] RODRÍGUEZ-CARVAJAL J., MARTÍNEZ J. L., PANNETIER J. and SAEZ-PUCHE R., *Phy. Rev. B*, **38** (1988) 7148; SAEZ-PUCHE R., FERNÁNDEZ F., MARTÍNEZ J. L. and RODRÍGUEZ-CARVAJAL J., *J. Less-Common Met.*, **149** (1989) 357.
[9] SAEZ-PUCHE R., RODRÍGUEZ J. L. and FERNÁNDEZ F., *Inorg. Chim. Acta*, **140** (1987) 151.
[10] BERTAUT E. F., *Acta Crystallogr., Sect. A*, **24** (1968) 217.
[11] RODRÍGUEZ-CARVAJAL J., FERNÁNDEZ-DÍAZ M. T., MARTÍNEZ J. L., SAEZ-PUCHE R. and FERNÁNDEZ F., *Phy. Rev. B*, to be submitted.
[12] LANDER G. H., BROWN P. J., HONIG J. M. and SPALEK J., *Phy. Rev. B*, **40** (1989) 4463.
[13] AXE J. D., MOUDDEN H., HOHLWEIN D., COX D. E., MOHANTY K. M., MOODENBAUGH A. R. and YOUWEN XU, *Phy. Rev. Lett.*, **62** (1989) 2751.
[14] HATCH D. M., STOKES H. T., ALEXANDROV K. S. and MISYUL S. V., *Phy. Rev. B*, **39** (1989) 9282, and references therein.
[15] MARTÍNEZ J. L. *et al.*, to be published.